STM JOURNALS

International Journal of
Molecular Biotechnological Research

Volume 1, Issue 1, 2023
DOI (Journal): *10.37591/IJMBR*

https://journals.stmjournals.com/ijmbr/

Research **IJMBR**

In Silico Molecular Docking of *Indigofera tinctoria* Phytocompounds to Target EGFR/ERK and FGFR/FGF Pathway Proteins Involved in Prostate Cancer

Nidhi Premanand Honavar*

Abstract

Objective: *Prostate cancer being the second major cause of cancer-related deaths in males, affects the small walnut-shaped gland below the bladder called the prostate gland. The epidermal growth factor protein (EGFR), cascade protein (ERK), and fibroblast growth factor proteins (FGFR and FGF) are involved in the different signaling pathways that lead to the formation of different products, that are responsible for the progression of cancer and thus can be considered as the therapeutic targets. Indigofera tinctoria, a medicinal plant with proven anti-cancerous properties, was chosen for this study to investigate its different compound's therapeutic effects against the target proteins, which are responsible for prostate cancer.* ***Methods:*** *In this study, 20 different compounds were selected from the Indigofera tinctoria plant as ligands to check for their binding affinity against the target proteins (EGFR, ERK, FGFR, and FGF). The docking of the ligands with the target proteins was done by using the PyRx Virtual tool. The computational investigation of all the ligands and the target proteins, such as their molecular structure, phytochemistry, therapeutic actions, and other data was carried out. The protein structure validation and the pharmacological evaluation of the ligands were done using the BIOVIA Discovery Studio, pdb sum generate, and ADMET lab 2.0, respectively.* ***Result:*** *The results of this study showed that the compounds, Pseudosemiglabrin, [(12S,15R,16R)-14,14-dimethyl-6-oxo-4-phenyl-3,11,13-trioxatetracyclo [8.6.0.02,7.012,16] hexadeca-1(10),2(7),4,8-tetraen-15-yl] acetate, Deguelin, Sumatrol and Rotenone showed good binding affinity with the target proteins and can be considered as a potential drug for the prostate cancer.* ***Conclusion:*** *The compounds selected were found to be active against the target proteins for prostate cancer and thus can be utilized for cancer suppression. Further in vitro studies need to be done to support this study.*

Keywords: Prostate cancer, molecular docking, *Indigofera tinctoria*, epidermal growth factor receptors, fibroblast growth factor receptors, extracellular regulated kinase, ADMET lab 2.0

INTRODUCTION

Prostate cancer is the second most common type of cancer found relevantly in males. It is the type of cancer that affects the small, soft, walnut-shaped gland found below the bladder in men, which helps in secreting seminal fluid and in male reproduction. It also secretes a few enzymes, lipids, amines, and metal ions which are very much essential for the normal growth and function of spermatozoa. According to Globocan (Global Cancer Observatory), it was estimated that in 2018, 1,276,106 new cases of prostate cancer and about 358,989 deaths were reported worldwide with higher prevalence in the developed countries [1]. The chances of occurrence of prostate cancer increase after the age of 50. It also depends on the family history.

EGFR (epidermal growth factor receptor) is an intercellular membrane protein that belongs to the

***Author for Correspondence**
Nidhi Premanand Honavar
E-mail: nidhihonavar26@gmail.com

Student, Department of Biotechnology, Indian Academy Degree College Autonomous, Hennur, Bangalore, Karnataka, India

Received Date: March 02, 2023
Accepted Date: April 02, 2023
Published Date: April 18, 2023

Citation: Nidhi Premanand Honavar. In Silico Molecular Docking of *Indigofera tinctoria* Phytocompounds to Target EGFR/ERK and FGFR/FGF Pathway Proteins Involved in Prostate Cancer. International Journal of Molecular Biotechnological and Research. 2023;1(1): 34–56p.

family of receptor tyrosine kinases (RTKs) [2]. Previous research has proved that the EGRF proteins are involved in the development of different types of cancers and pathogenesis, thus being the most prominent target for anti-cancer drugs [3, 4]. These transmembrane proteins are activated by peptide growth factors. Upon activation, EGFR proteins get phosphorylated and lead to the network of signal transduction pathways with the help of other transmembrane receptor proteins [5, 6]. The activated EGFR protein further activates mitogen-activated protein kinase pathway (MAPK or MEK) and extracellular regulated kinase (ERK) pathway in prostate cancer.

FGF (fibroblast growth factor), and the receptor FGFR (fibroblast growth factor receptor) have many different functions, such as embryonic development, differentiation, proliferation, survival, migration, and angiogenesis. The typical regulation of the FGF/FGFR system occurs in multiple human tumors, leading to the deregulated activation of ligand-dependent or -independent FGFR signaling [4]. FGFRs are widely expressed in developing and adult tissues and have various biological activities both in vivo and in vitro, including roles in angiogenesis, mitogenesis, cellular differentiation, cell migration, and tissue injury repair [7]. The FGF and FGFR proteins interact with each other on the cell surface with the mediations of Heparin Sulphate Proteoglycans (HSPGs) which are available on the cell surface and form the ternary complex HSPGD/FGF/FGFR, necessary for triggering the signal transduction pathways [5].

Indigofera tinctoria is a branching shrub, that belongs to Fabaceae family, widely distributed in tropical regions [8]. The Phytochemical constituents of *Indigofera tinctoria* are mainly responsible for its wide therapeutic actions such as liver disease, heart palpitations, and gout, and have laxative properties. It is used in traditional medicines, Ayurveda, Siddha, and Unani Studies conducted on *Indigofera tinctoria* showed that it possesses cytotoxic effects, Anti-bacterial, Antioxidant, Anti-inflammatory, anti-hepatoprotective and Antidiabetic activity [9]. Some of the compounds found in the plant, such as deguelin, pseudosemiglabrin, indirubin, tephrosin, and kaempferol are proven to be having anti-cancerous properties and help in curing various diseases [10–15].

METHODOLOGY

Retrieval of the Ligands

The ligands from the plant *Indigofera tinctoria* were selected for the study. For the retrieval of the ligands, the IMPPAT website was used (*https://cb.imsc.res.in/imppat/home*). A total of 20 ligands were selected. The PubChem ID and the canonical SMILES were noted from the PubChem website (*https://pubchem.ncbi.nlm.nih.gov/*). The ligands were downloaded in 2D SDF format [16].

Retrieval of the Protein

The target proteins (4zzm, 5b7v, 2p23, 1m17) were searched on the RCSB PDB website (*https://www.rcsb.org/*). The proteins were downloaded in pdb format. These proteins were added with their missing residues using BIOVIA Discovery Studio [6].

Purification of the Protein

The proteins were purified by removing the water molecules, Het atoms, ligand groups, and additional chains apart from the A chain. For the proper binding of the protein with the ligand without the free energy disturbances from the water molecules. The protein purification was done using Discovery BIOVIA [17]. The purified proteins were subjected to PDB Sum generate (*https://www.ebi.ac.uk/thornton-srv/databases/pdbsum/Generate.html*) where the secondary structure and the Ramachandran plot of the proteins were obtained.

Molecular Docking and Visualization

The molecular docking of the ligands with the proteins was done one by one using PyRx Software. These proteins were added as macromolecules with the compounds from plants as ligands. The energy

minimization step was done, and the selected ligands were converted into .pdbqt format [18]. These selected ligands were docked with all the selected proteins. The interactions of the ligands with the proteins were interpreted by considering their binding energy scores. The binding energy score corresponding to 0 RMSD (root mean square deviation) was taken into consideration as the best docking conformation. The top 6 conformations with the least binding conformations from each protein were taken into consideration as the best complex for the target protein [19]. The .pdb files of the top 6 docked ligand structures were downloaded and visualized in BIOVIA Discovery Studio.

The selected top ligands of the respective proteins in their respective conformations were downloaded in the .pdb format from the PyRx and visualized in the BIOVIA Discovery Studio. The ligands were pasted in purified protein structures. The 3D structure, 2D structure, and the non-bond interactions were documented.

Pharmacological Studies

The pharmacological analysis of the ligands was done using the ADMET lab 2.0 web server. It is an integrated online web tool for the prediction of the accurate adsorption, desorption, metabolism, elimination, and toxicity parameters of the compounds [20]. Physiochemical properties including molecular weight, lipophilicity, saturation, etc., and the toxicity parameters were also tabulated and evaluated.

RESULTS

Selection of the Phytocompounds

The plant *Indigofera tinctoria* is known for its medicinal properties and the studies suggest that it has good anti-cancerous properties, effective against colon cancer, lung cancer [17], and ovarian cancer. 20 ligands were selected from the IMPPAT website. The 2D structures of the ligands were downloaded from the PubChem website in SDF format (Table 1). The structures were viewed using BIOVIA Discovery.

Table 1. Ligand name, PubChem ID, and Canonical SMILES of the 20 selected compounds.

S.N.	Ligand	PubChem ID	Canonical SMILES
1	Indigo	10215	C1=CC=C2C(=C1)C(=C(N2)C3=NC4=CC=CC=C4C3=O)O
2	Indican	441564	C1=CC=C2C(=C1)C(=CN2)OC3C(C(C(C(O3)CO)O)O)O
3	Kaempferol	5280863	C1=CC(=CC=C1C2=C(C(=O)C3=C(C=C(C=C3O2)O)O)O)O
4	Indicine	73615	CC(C)C(C(C)O)(C(=O)OCC1=CCN2C1C(CC2)O)O
5	D-Galactose	6036	C(C1C(C(C(C(O1)O)O)O)O)O
6	Tephrosin	114909	CC1(C=CC2=C(O1)C=CC3=C2OC4COC5=CC(=C(C=C5C4(C3=O)O)OC)OC)C
7	Rotenone	6758	CC(=C)C1CC2=C(O1)C=CC3=C2OC4COC5=CC(=C(C=C5C4C3=O)OC)OC
8	Sumatrol	442824	CC(=C)C1CC2=C(O1)C=C(C3=C2OC4COC5=CC(=C(C=C5C4C3=O)OC)OC)O
9	Apigenin	5280443	C1=CC(=CC=C1C2=CC(=O)C3=C(C=C(C=C3O2)O)O)O
10	Luteolin	5280445	C1=CC(=C(C=C1C2=CC(=O)C3=C(C=C(C=C3O2)O)O)O)O
11	Indirubin	10177	C1=CC=C2C(=C1)C(=C(N2)O)C3=NC4=CC=CC=C4C3=O
12	Dehydrodeguelin	3083803	CC1(C=CC2=C(O1)C=CC3=C2OC4=C(C3=O)C5=CC(=C(C=C5OC4)OC)OC)C
13	Coumarin	323	C1=CC=C2C(=C1)C=CC(=O)O2

S.N.	Ligand	PubChem ID	Canonical SMILES
14	Deguelin	107935	CC1(C=CC2=C(O1)C=CC3=C2OC4COC5=CC(=C(C=C5C4C3=O)OC)OC)C
15	Pseudosemiglabrin	156341	CC(=O)OC1C2C(OC3=C2C4=C(C=C3)C(=O)C=C(O4)C5=CC=CC=C5)OC1(C)C
16	1 H-indol-3-ol	50591	C1=CC=C2C(=C1)C(=CN2)O
17	[(12S,15R,16R)-14,14-dimethyl-6-oxo-4-phenyl-3,11,13-trioxatetracyclo[8.6.0.02,7.012,16]hexadeca-1(10),2(7),4,8-tetraen-15-yl] acetate	182678	CC(=O)OC1C2C(OC3=C2C4=C(C=C3)C(=O)C=C(O4)C5=CC=CC=C5)OC1(C)C
18	D-Mannose	18950	C(C1C(C(C(C(O1)O)O)O)O)O
19	Galactomannan	439336	C(C1C(C(C(C(O1)OCC2C(C(C(C(O2)O)O)O)OC3C(C(C(C(O3)CO)O)O)O)O)O)O)O
20	Rotenol	44257420	CC(=C)C1CC2=C(O1)C=CC(=C2O)C(=O)C3CCOC4=CC(=C(C=C34)OC)OC

Protein Structure Analysis

Ramachandran Plot and Ramachandran Plot Statistics

The Ramachandran plot of the proteins 1M17, 4ZZM, 5B7V, and 2P23 were obtained with the help of the 'PDB Sum Generate' website, as shown in Figure 1, Figure 2, Figure 3, and Figure 4 respectively.

1M17

For the purified protein 1M17, when subjected to pdb sum generate, the results showed that 79.8% of the residues were in the most favored region, 18.1% of the residues in the additional favored region, and 0.3% in the generously favored option. 1.7% of the residues were found to be in the disallowed regions (Figure 1).

4ZZM

86.4% of its residues of the protein 4ZZM fall under the most favored regions. 8.3% of residues fall under additional allowed regions. 3.0% in generously allowed regions and the remaining 2.3% of the residues in disallowed regions (Figure 2).

5B7V

Likewise, 5B7V protein had 87.3% of its residues in the most favored regions, 12.0% in additional allowed regions, and 0.6% in the generously allowed regions (Figure 3).

2P23

The Ramachandran plot for the protein 2p23 showed that 92.2% of the residues fall under the most favored regions. 6.9% of residues fall under additional allowed regions. And the remaining 0.9% of the residues in generously allowed regions (Figure 4).

These results suggest that the purified 3D models of the proteins are good quality models.

Secondary Structure

The pdb sum produced the secondary structures of the proteins namely 4zzm, 5b7v, 2p23, and 1m17, respectively, as shown in Figure 1, Figure 2, Figure 3, and Figure 4, respectively.

1M17

The PDB findings for the secondary structure suggested that the protein has 4 sheets, 5 beta hairpins, 4 beta bulges, 11 strands, 15 helices, 11 helix-helix, 22 beta turns, and 2 gamma turns. There are 324 residues in the structure.

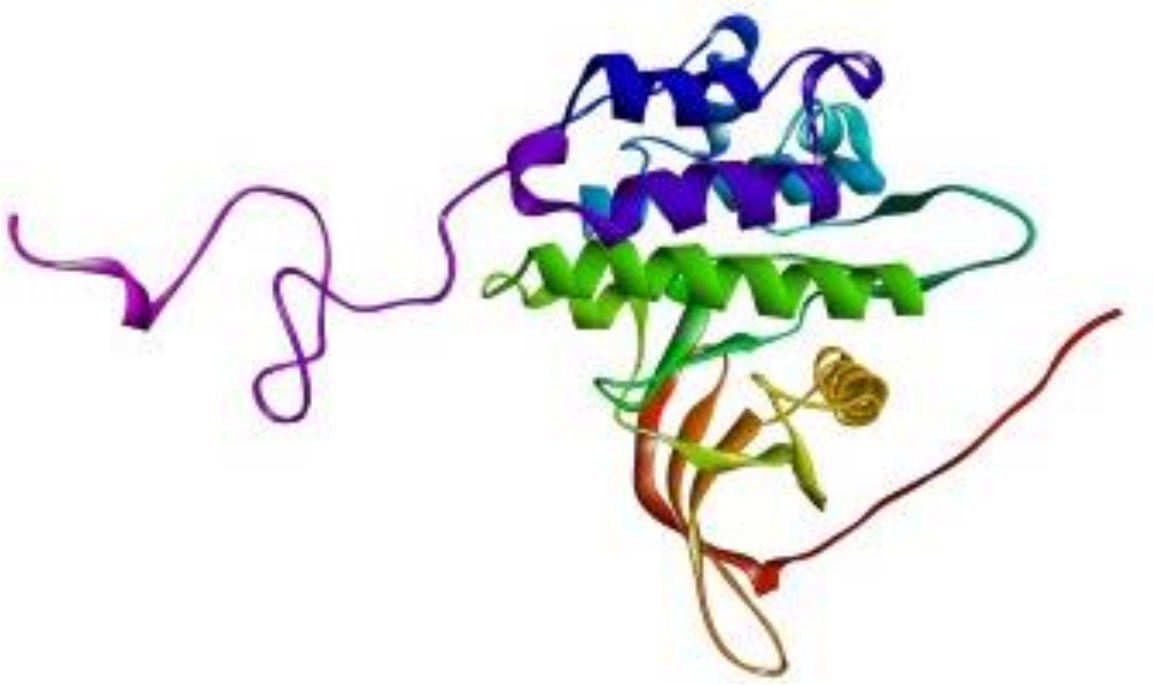

(a)

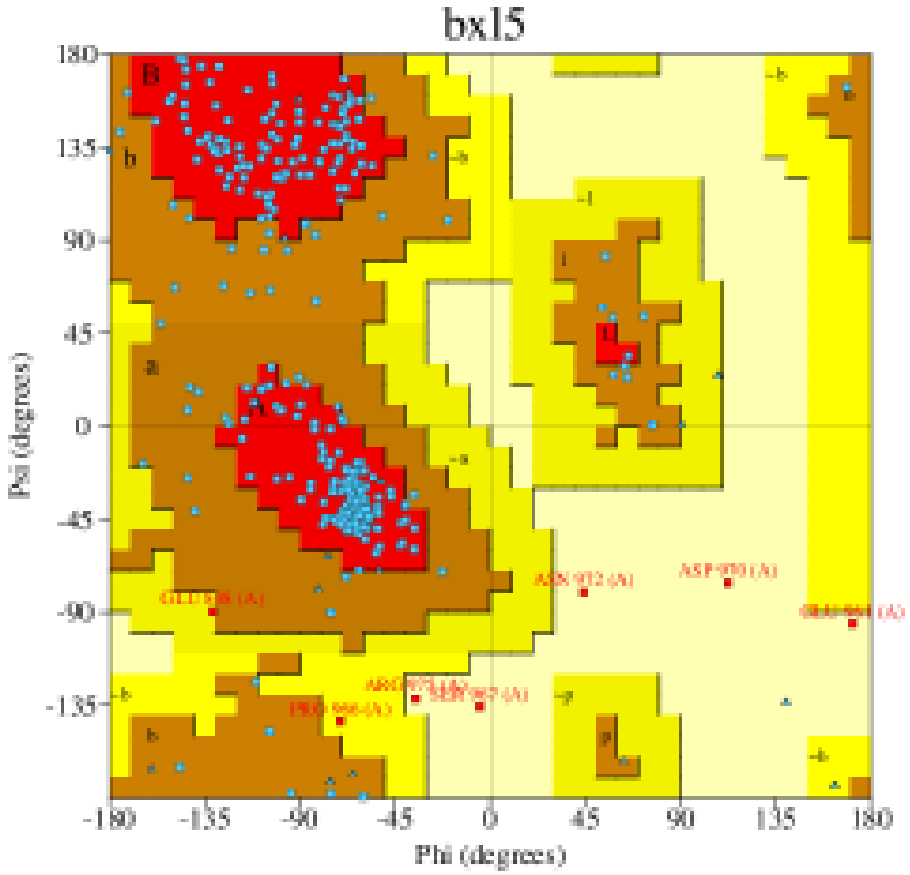

(b)

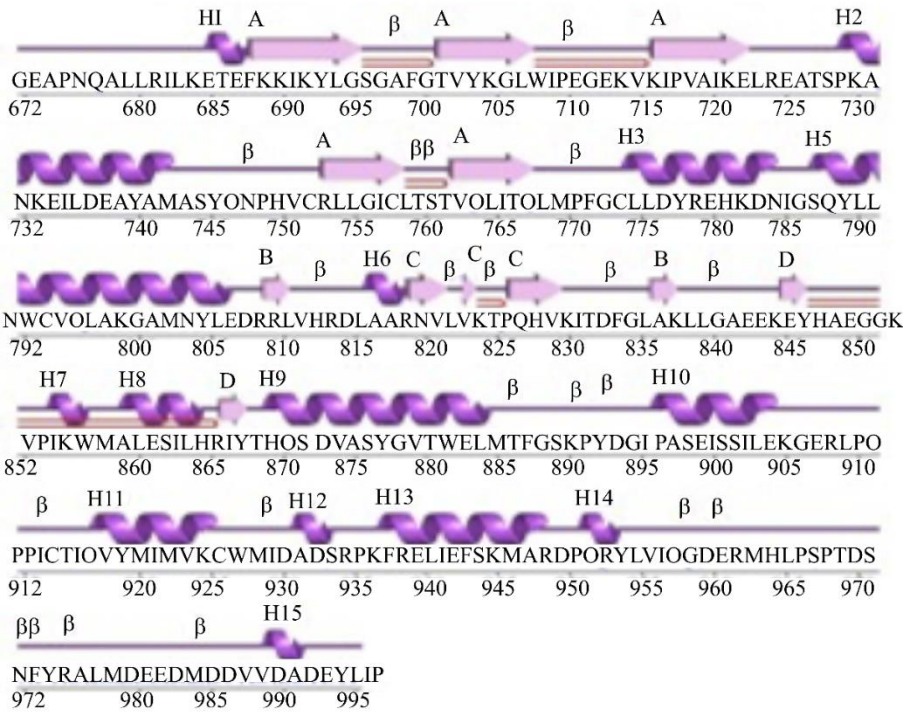

(c)

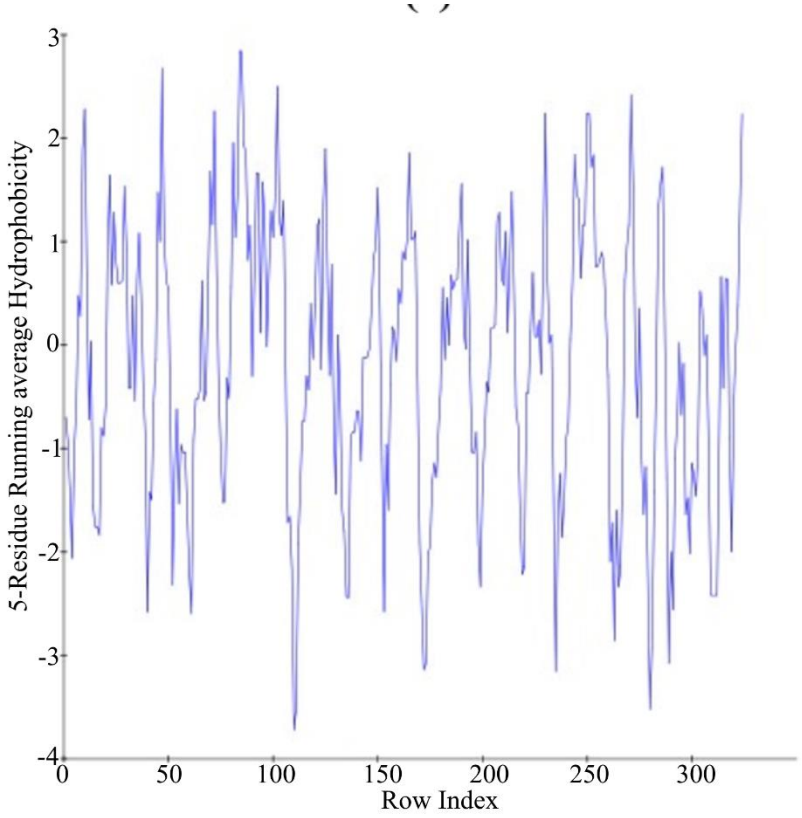

(d)

Figure 1. Structural analysis of 1M17 protein: (a) refers to purified 1m17 protein structure. (b) Ramachandra plot, (c) secondary structure of 4zzm protein, and (d) hydropathy plot.

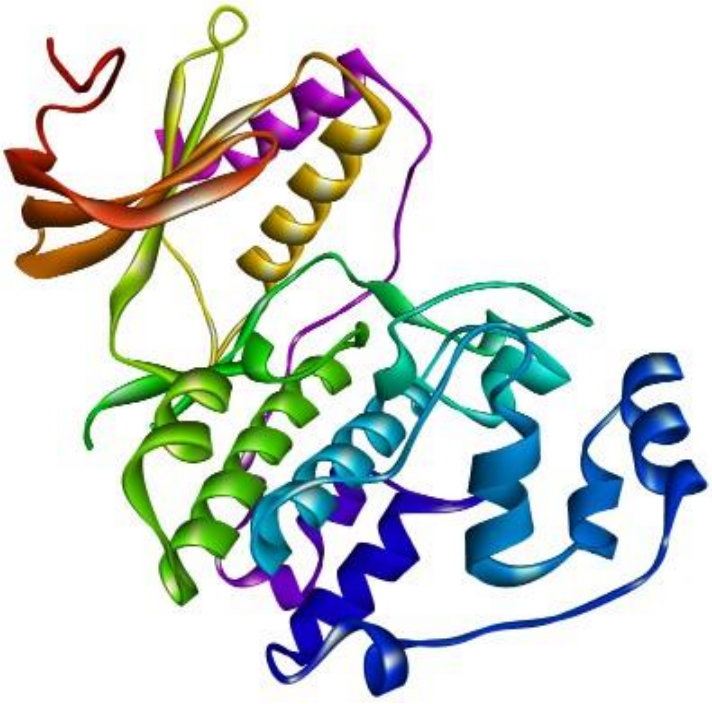

(a)

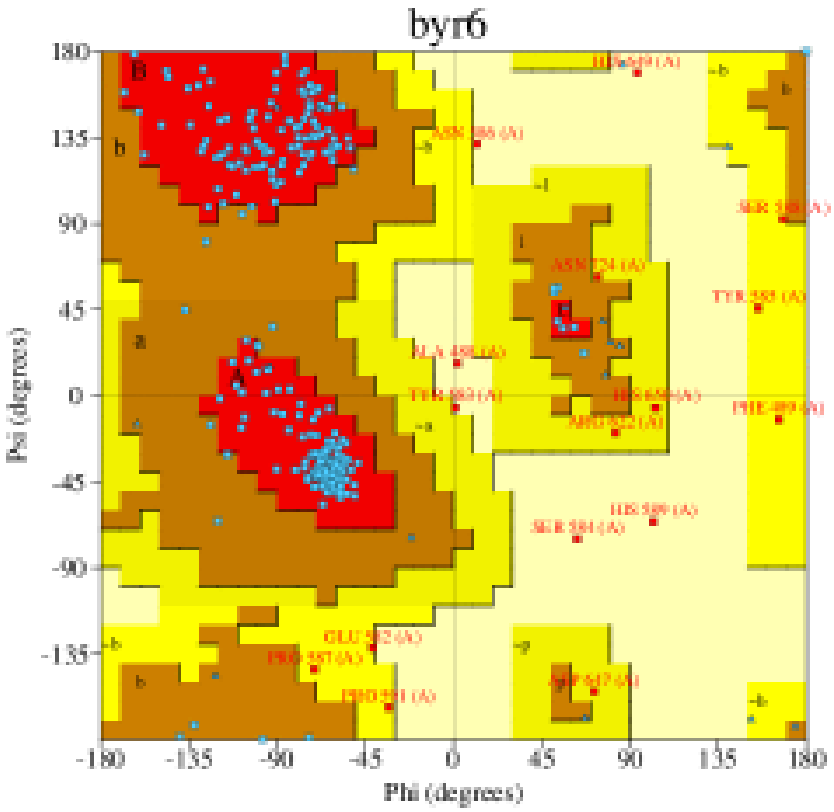

(b)

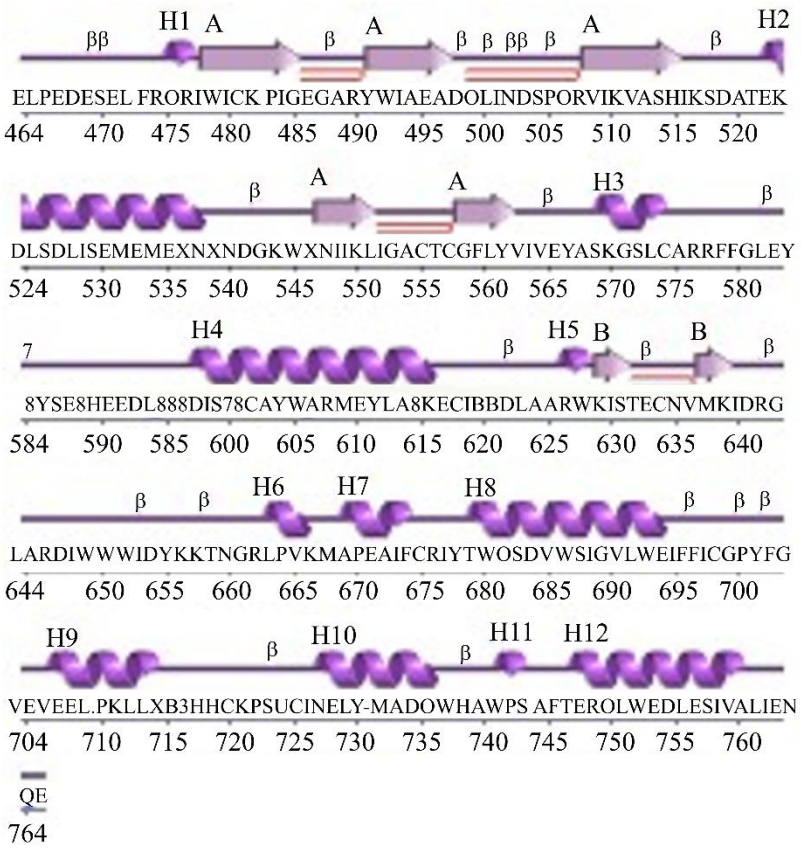

(c)

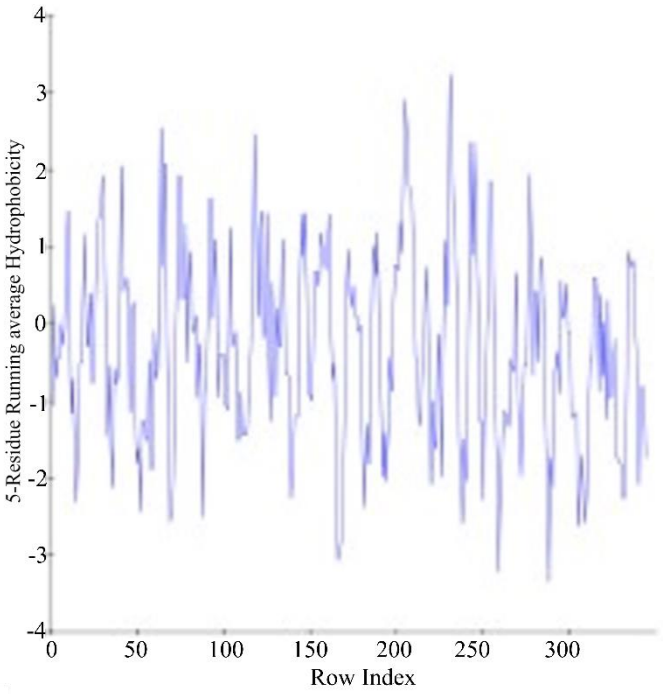

(d)

Figure 2. Structural analysis of 4ZZM protein: (a) refers to purified 4zzm protein structure. (b) Ramachandra plot, (c) secondary structure of 4zzm protein, and (d) hydropathy plot.

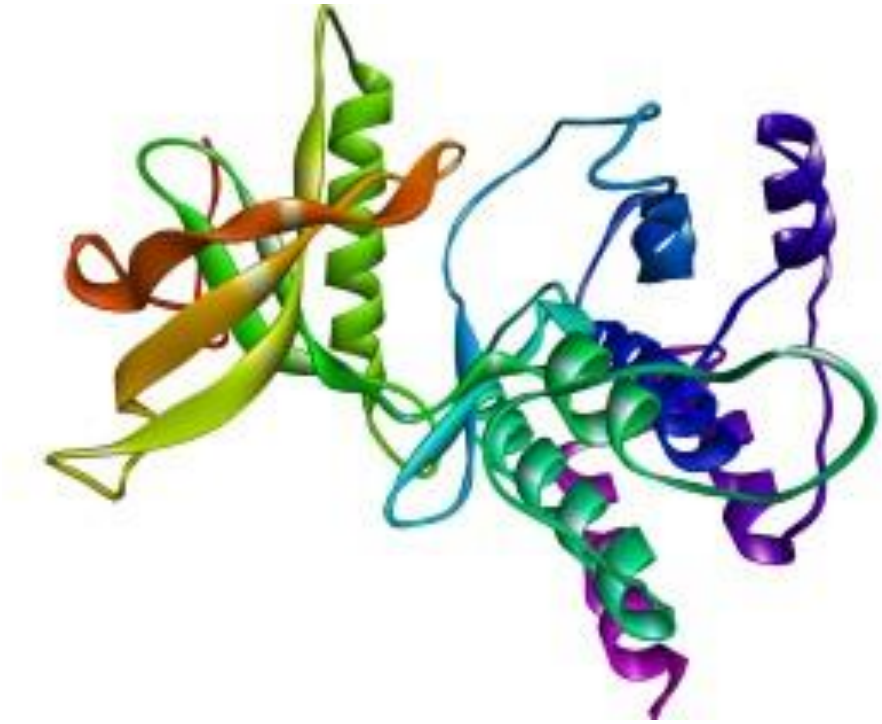

(a)

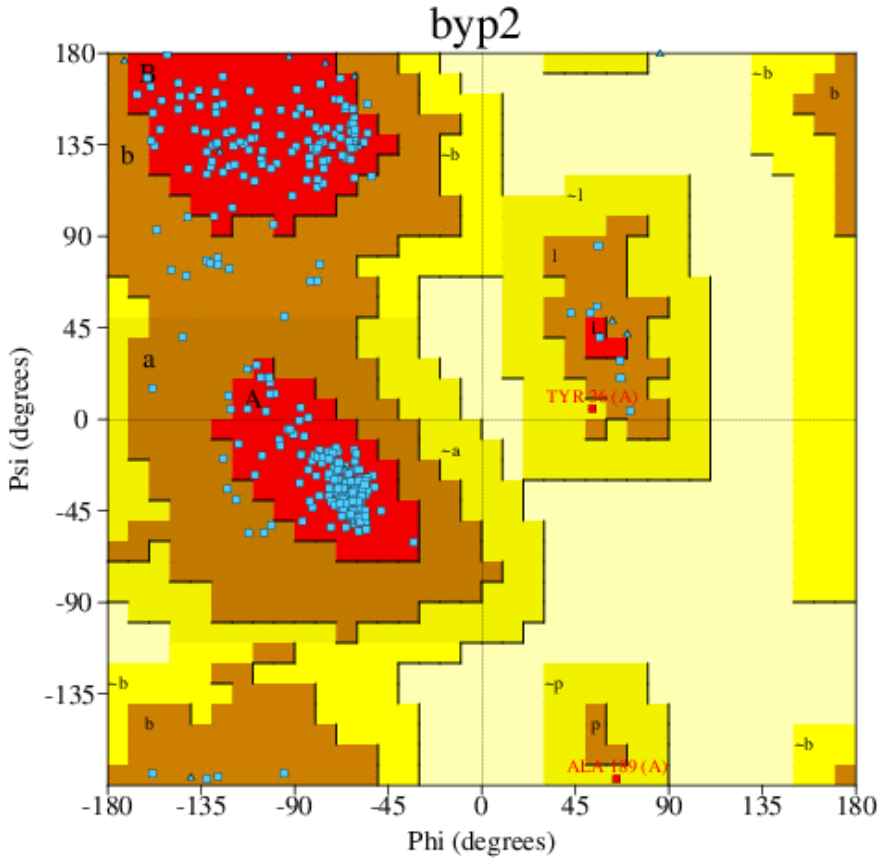

(b)

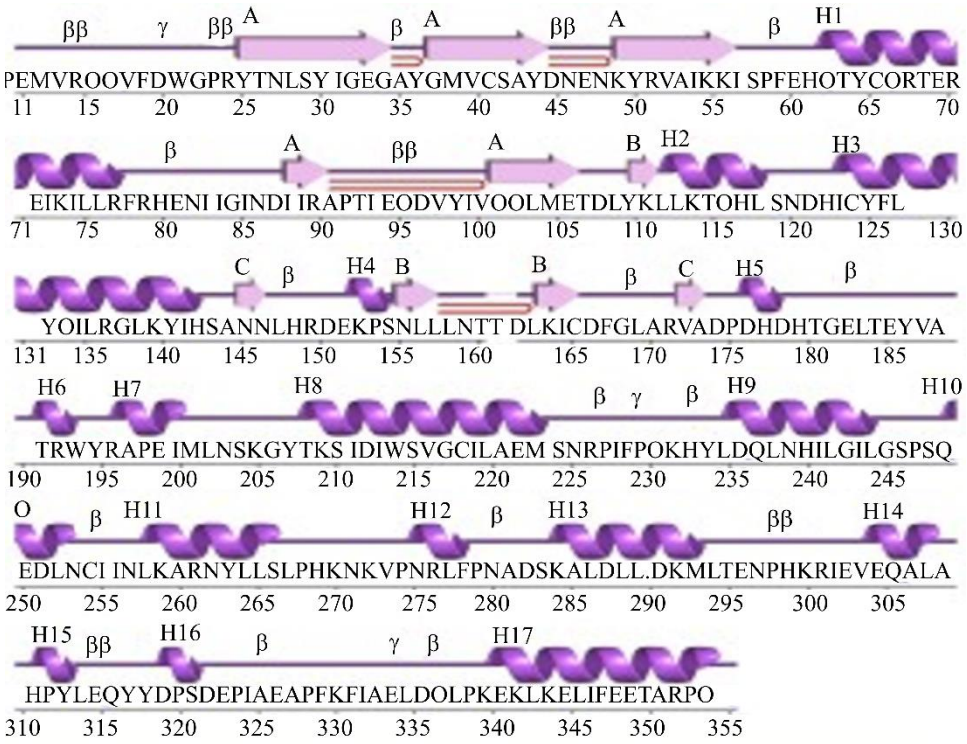

(c)

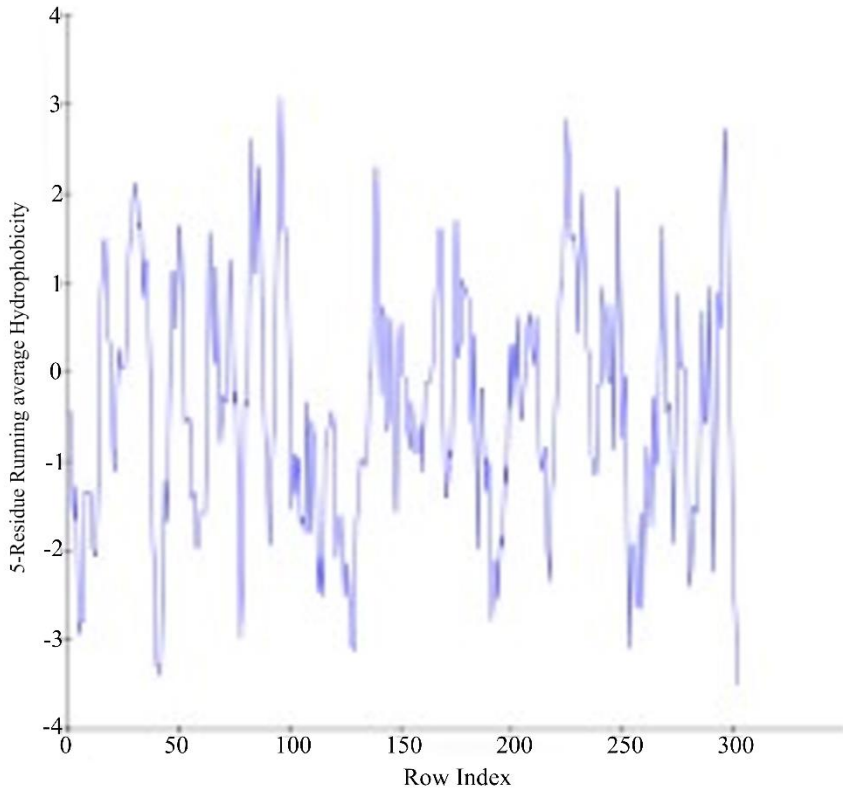

(d)

Figure 3. Structural analysis of 5B7V protein: (a) refers to purified 5b7v protein structure. (b) Ramachandra plot, (c) secondary structure of 4zzm protein, and (d) hydropathy plot.

4ZZM

In the case of 4ZZM, the pdb sum result depicted are 2 sheets, 4 beta hairpins, 4 beta bulges, 7 strands, 12 helices, 15 helix-helix, 22 beta turns, and 1 gamma turn. The protein contains 302 residues.

5B7V

For 5B7V, the pdb sum data showed 3 sheets, 4 beta hairpins, 5 beta bulges, 10 strands, 18 helices, 18 helix-helix, 24 beta turns, and 3 gamma turns. The structure consisted of 344 residues in total.

2P23

Finally, the pdb sum outputs of the 2P23 protein are 2 sheets, 6 beta hairpins, 5 beta bulges, 11 strands, 4 helices, 16 beta turns, and 2 disulfides. The structure comprises 136 residues in total.

Hydropathy Plots

The hydropathy plots of the proteins 1M17, 4ZZM, 5B7V, AND 2P23 were investigated using the BIOVIA Discovery Studio software, as shown in Figure 1 Figure 2, Figure 3, and Figure 4, respectively.

Molecular Docking and Visualization

The docking of the 20 ligands with the 4 protein targets was done using the PyRx Software. The ligands with the lowest binding energy with respect to the zeroth value of the RMSD were chosen as the best docking conformation of the protein targets. Once the docking of the ligand with the protein targets was done, the binding affinity and the RMSD/ub and RMSD/lb were documented. Among the 20 ligands screened, the top 6 ligands which had the lowest binding energy with the proteins namely 1m17 (Figures 5 and 6), 4zzm (Figures 7 and 8), 5b7v (Figures 9 and 10), and 2p23 (Figures 11 and 12) respectively were subjected to visualization using BIOVIA Discovery Studio Visualizer. The 3-dimensional and 2-dimensional models were acquired. Furthermore, the details of the non-bond interactions were also documented.

- Visualization of 1M17:
- Visualization of 4ZZM:
- Visualization of 5B7V:
- Visualization of 2P23:

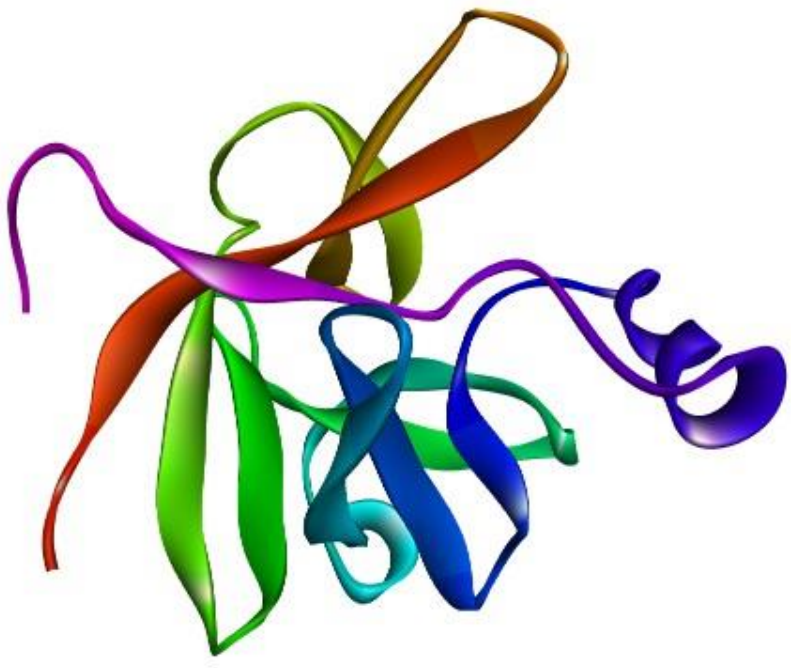

(a)

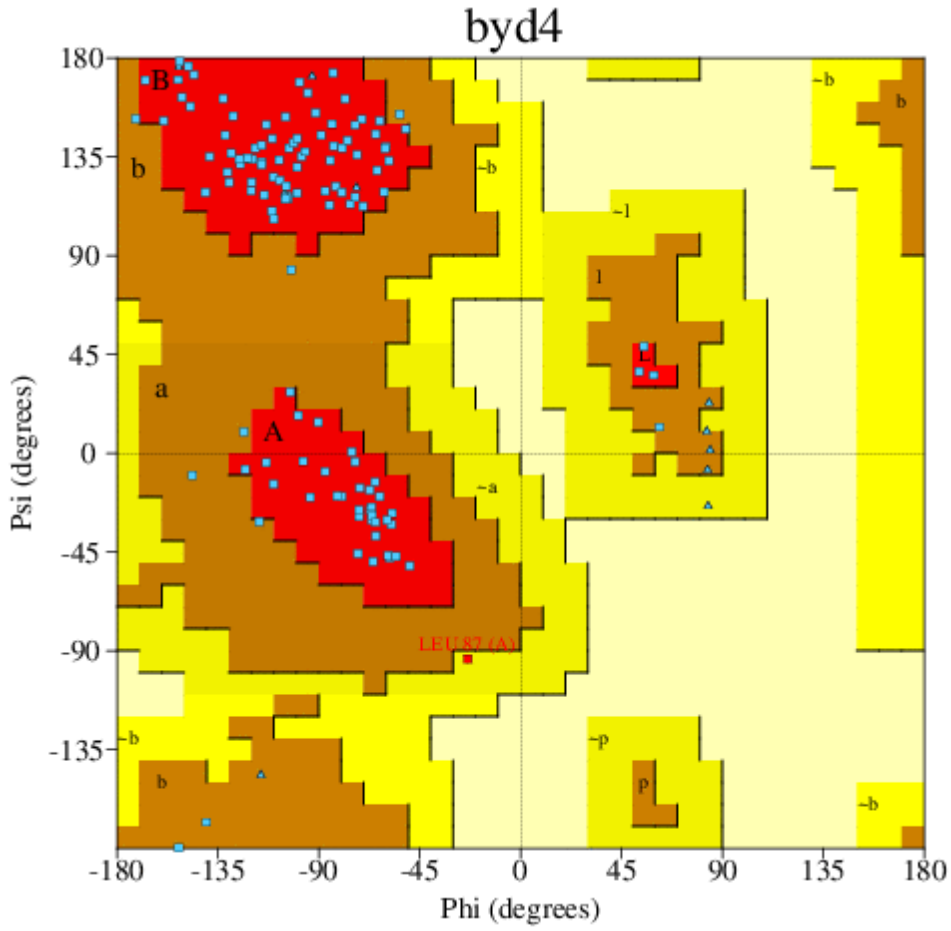

(b)

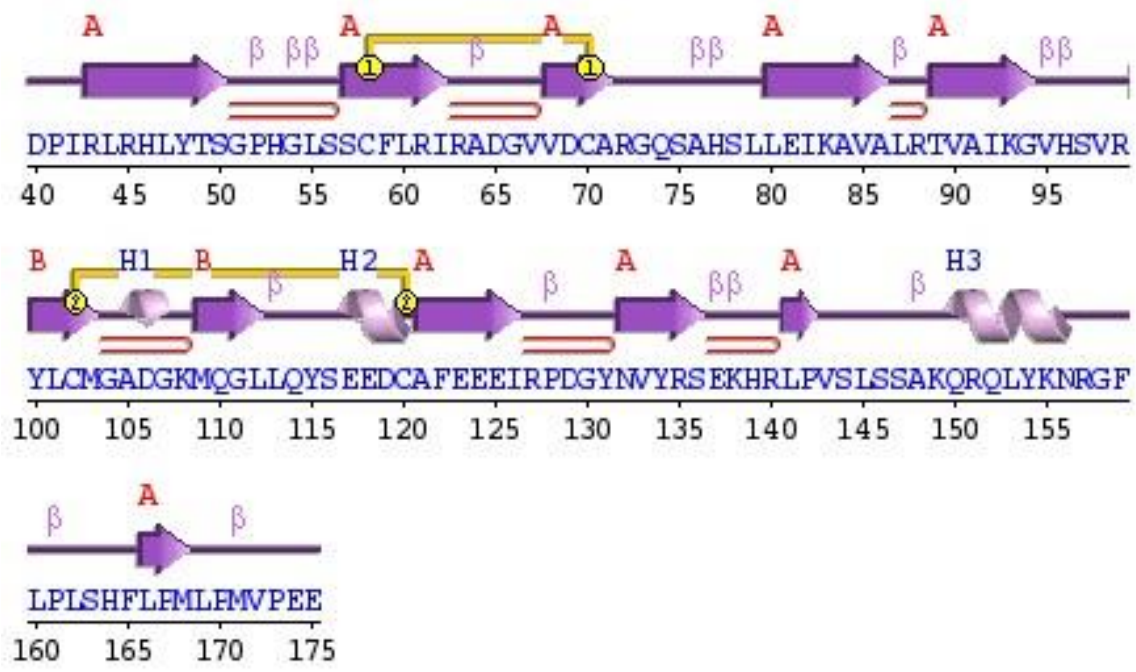

(c)

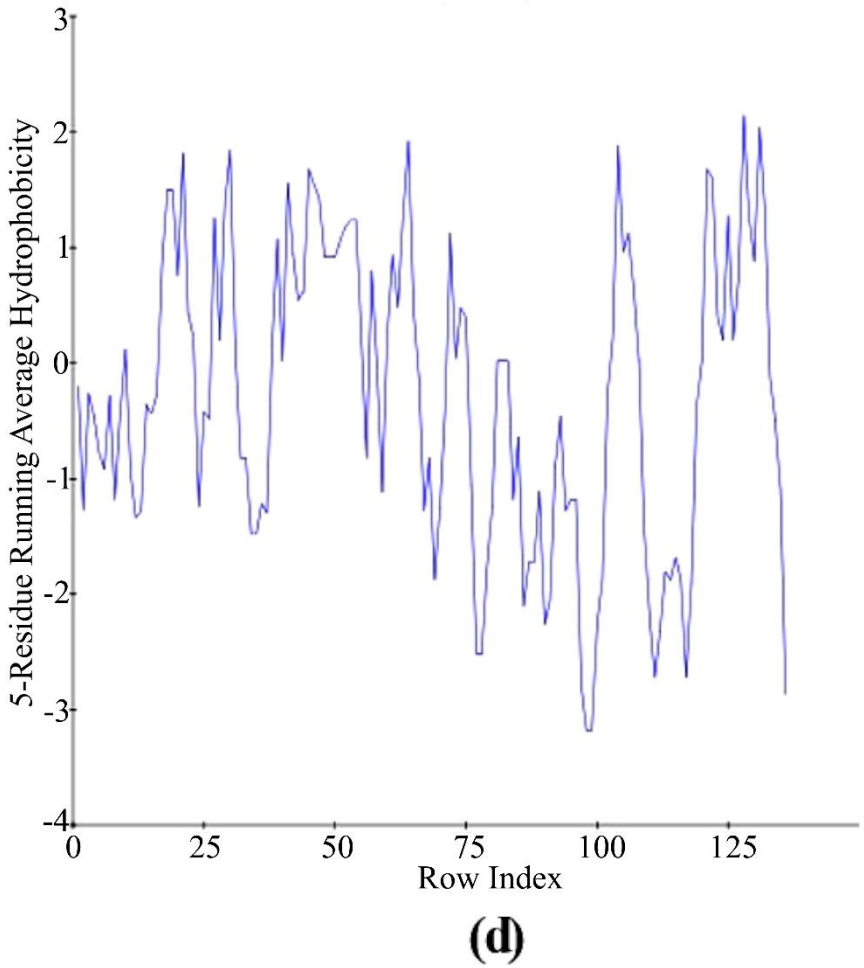

Figure 4. Structural analysis of 2P23 protein: (a) refers to purified 2p23 protein structure. (b) Ramachandra plot, (c) secondary structure of 4zzm protein, and (d) hydropathy plot.

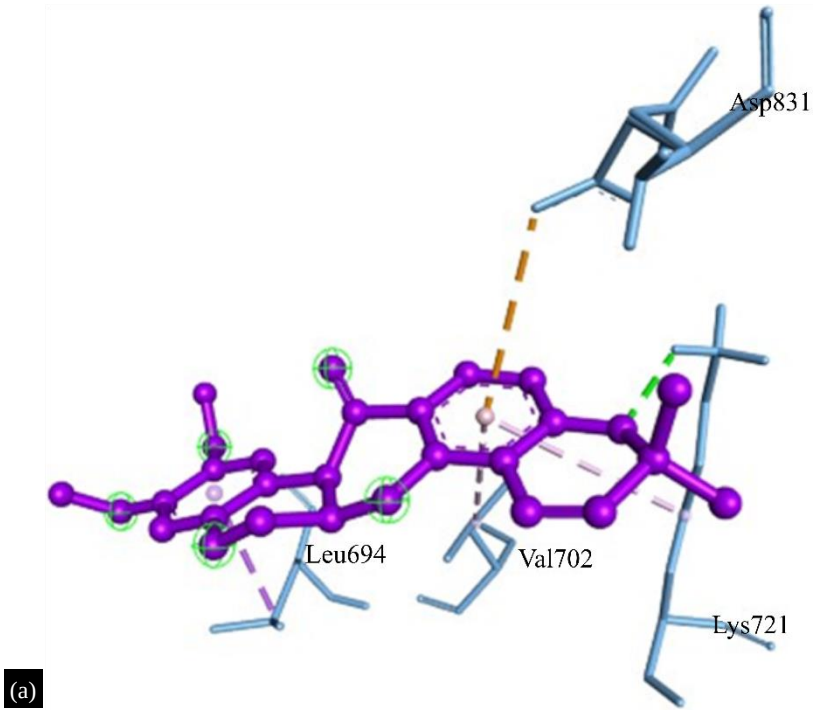

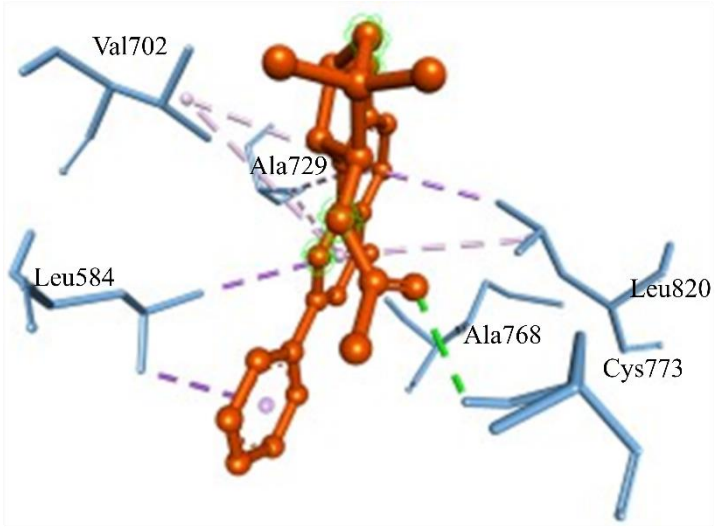

(b)

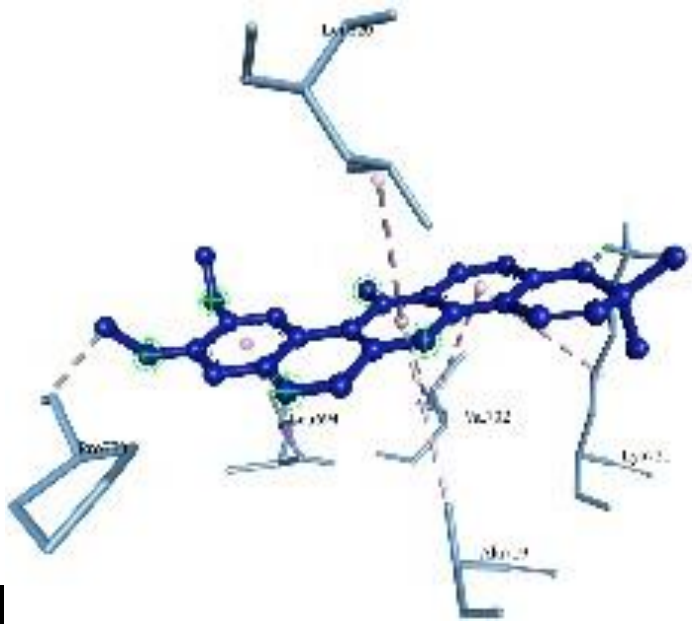

(c)

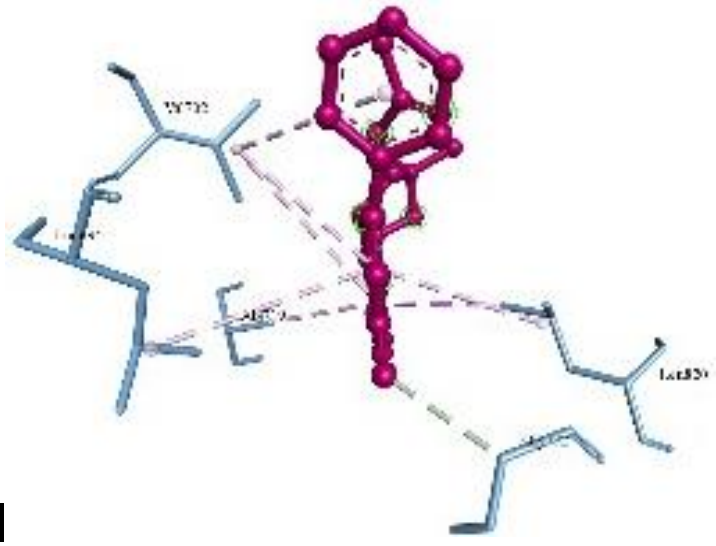

(d)

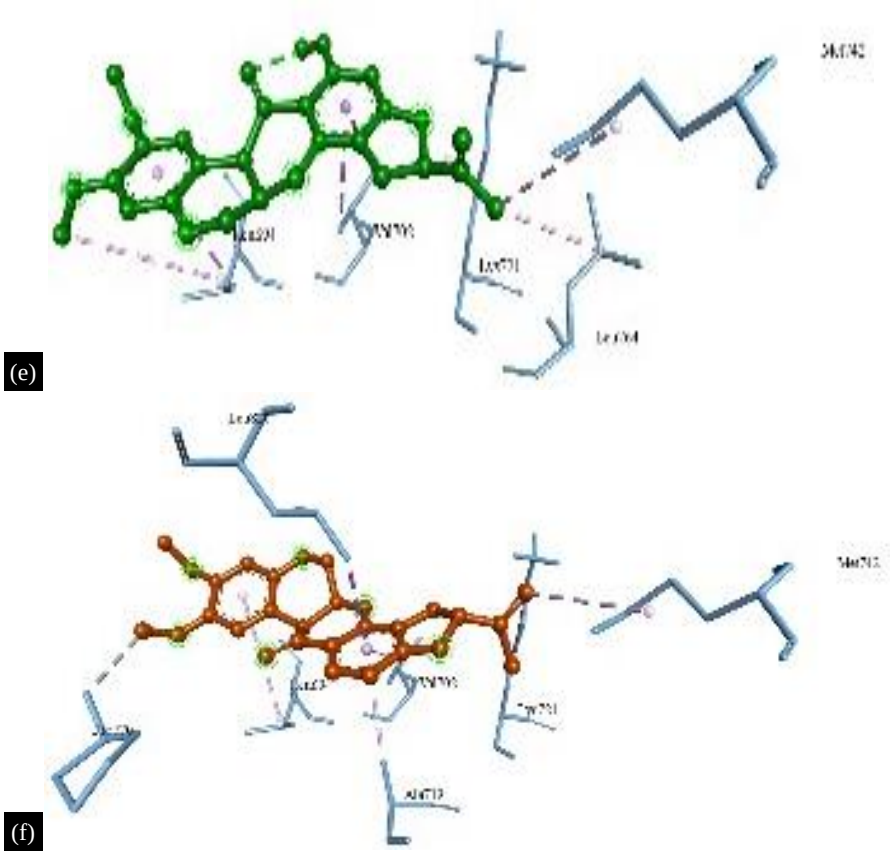

Figure 5. 3D interactions of top ligands interacting with 1M17 protein.

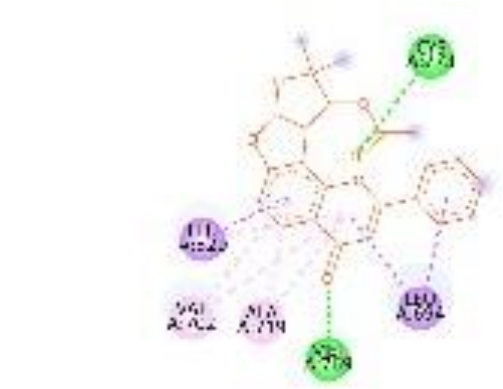

(b)

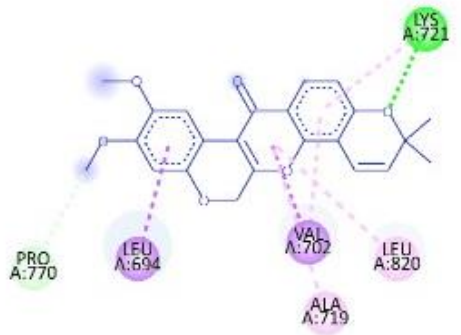

(c)

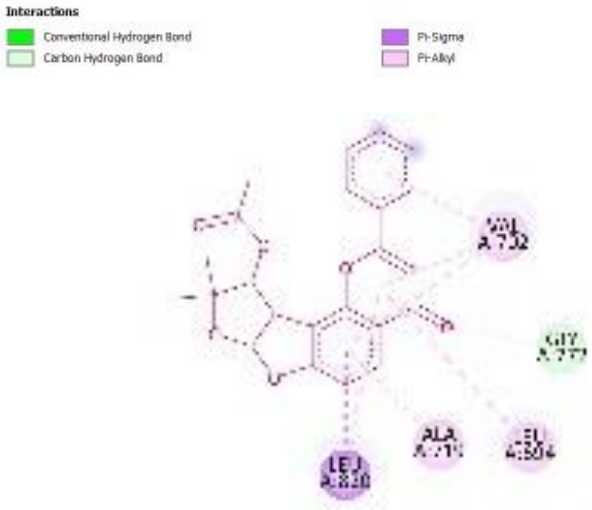

(d)

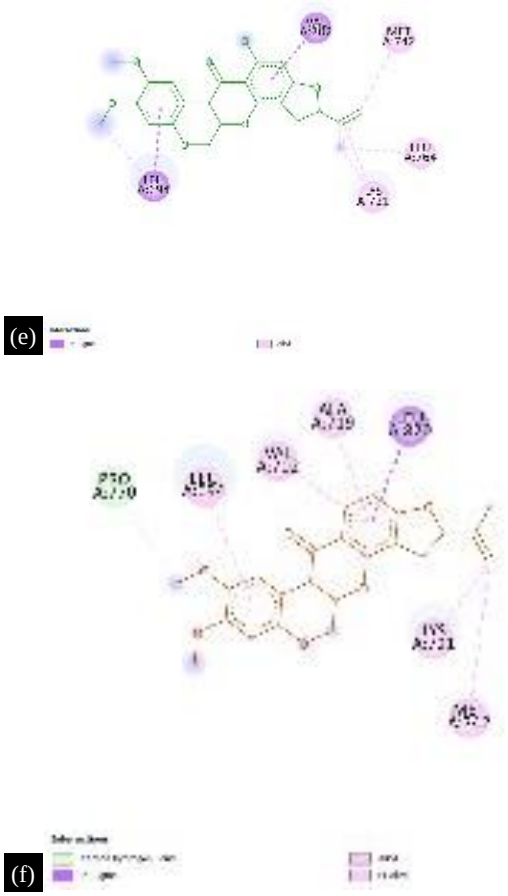

Figure 6. 2D interactions of top ligands interacting with 1M17 protein.

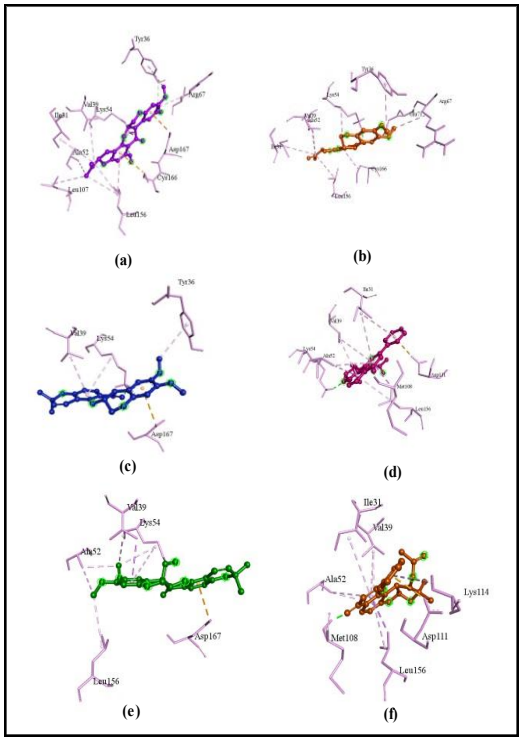

Figure 7. 3D interactions of top ligands interacting with 4ZZM protein.

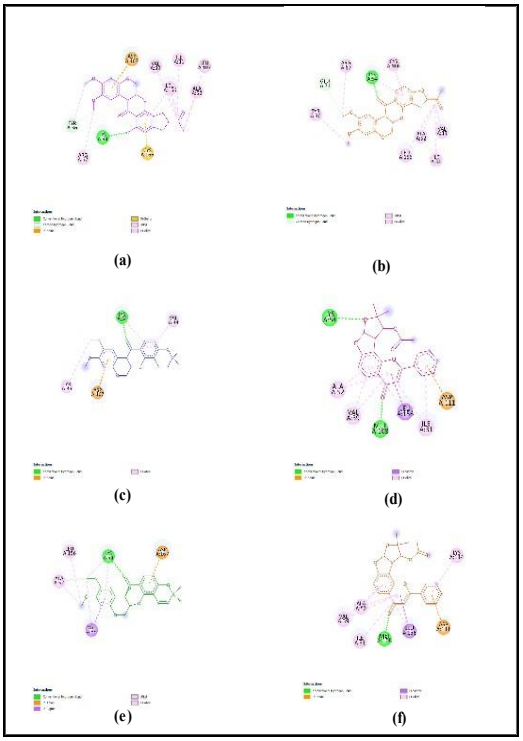

Figure 8. 2D interactions of top ligands interacting with 4ZZM protein.

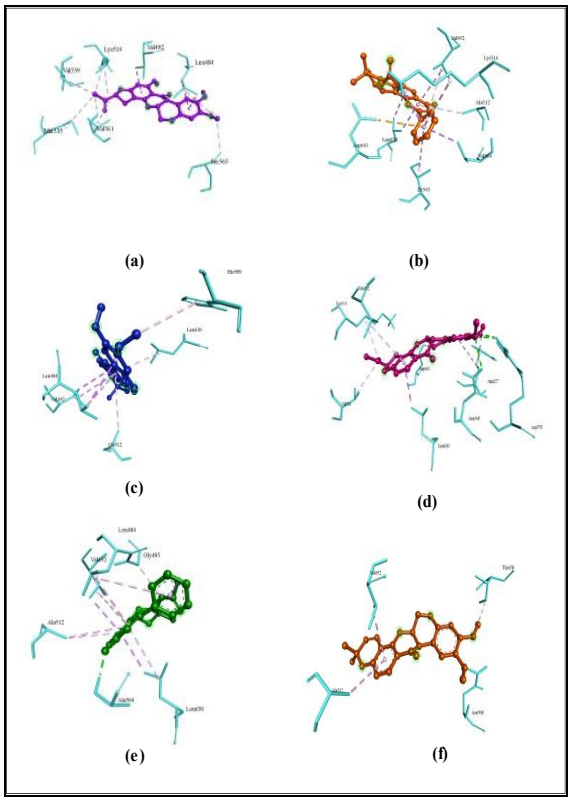

Figure 9. 3D interactions of top ligands interacting with 5B7V protein.

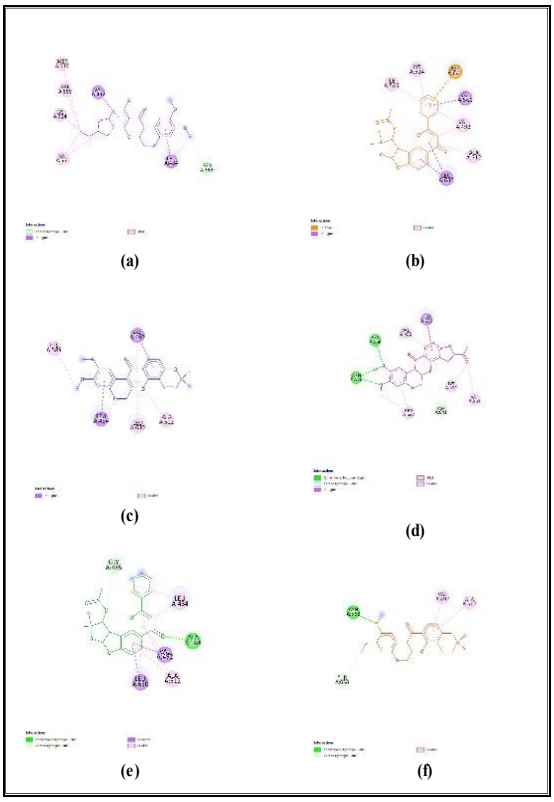

Figure 10. 2D interactions of top ligands interacting with 5B7V protein.

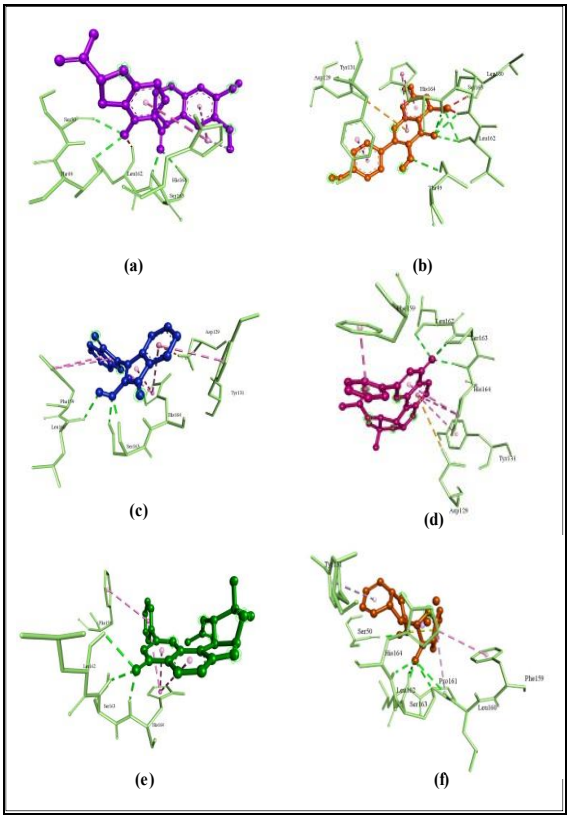

Figure 11. 3D interactions of top ligands interacting with 2P23 protein.

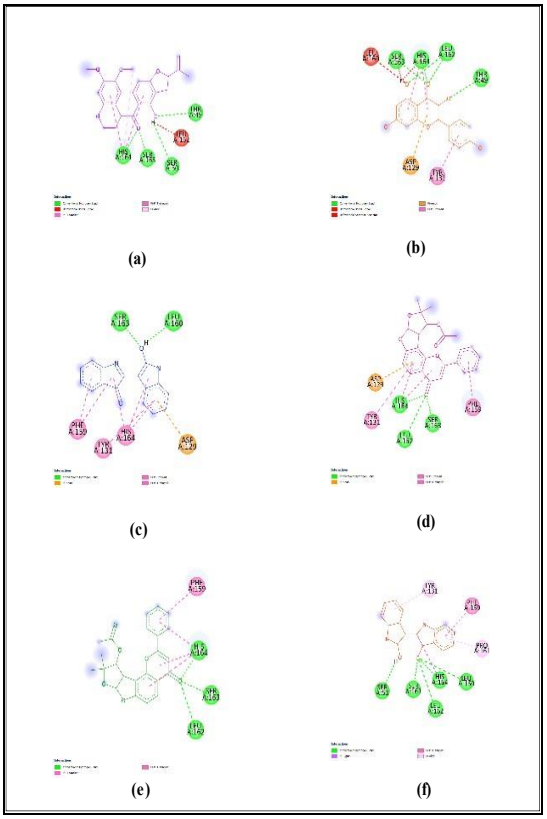

Figure 12. 2D interactions of top ligands interacting with 5B7V protein.

ADMET Analysis

The 6 ligands selected from each of the four proteins were screened for their adsorption, desorption, physiochemical properties, medicinal properties, and toxicity through the ADMET lab 2.0 web tool. The results are depicted as follows (Tables 2–7).

Table 2. Physiochemical properties of the top 15 ligands.

PubChem ID	MW	Vol	nHD	nHA	nRot	nRing	nHet	fChar	Flex	TPSA	LogS
442824	410.14	404.022	1	7	3	5	7	0	0.111	83.45	-5.114
107935	394.14	395.232	0	6	2	5	6	0	0.074	63.22	-4.469
156341	392.13	392.595	0	6	3	5	6	0	0.111	74.97	-4.504
182678	392.13	392.595	0	6	3	5	6	0	0.111	74.97	-4.504
3083803	392.13	392.595	0	6	2	5	6	0	0.074	67.13	-5.227
44257420	396.16	403.788	1	6	5	4	6	0	0.217	74.22	-5.296
6758	394.14	395.232	0	6	3	5	6	0	0.111	63.22	-5.497
10177	262.07	266.912	2	4	1	4	4	0	0.048	65.45	-4.653
114909	410.14	404.022	1	7	2	5	7	0	0.074	83.45	-4.623
5280445	286.05	273.977	4	6	1	3	6	0	0.056	111.13	-3.629
10215	262.07	266.912	2	4	1	4	4	0	0.048	65.45	-4.271
5280863	286.05	273.977	4	6	1	3	6	0	0.056	111.13	-3.624
5280443	270.05	265.186	3	5	1	3	5	0	0.056	90.9	-3.606
439336	504.17	434.858	11	16	7	3	16	0	0.389	268.68	0.414
441564	295.11	278.223	5	7	3	3	7	0	0.188	115.17	-2.172

Table 3. Medicinal chemistry of the top 15 ligands.

PubChem CID	QED	Synth	Fsp3	Lipinski	PAINS
442824	0.777	3.999	0.348	Accepted	0
107935	0.767	3.698	0.348	Accepted	0
156341	0.614	3.773	0.304	Accepted	0
182678	0.614	3.773	0.304	Accepted	0
3083803	0.637	3.056	0.261	Accepted	0
44257420	0.607	3.595	0.348	Accepted	0
6758	0.740	3.868	0.348	Accepted	0
10177	0.707	2.512	0	Accepted	0
114909	0.814	3.853	0.348	Accepted	0
5280445	0.511	2.420	0	Accepted	1
10215	0.707	2.487	0	Accepted	0
5280863	0.546	2.375	0	Accepted	0
5280443	0.632	2.253	0	Accepted	0
439336	0.154	4.839	1	Rejected	0
441564	0.514	3.514	0.429	Accepted	0

Table 4. Absorption properties of the top 15 ligands.

PubChem CID	Caco-2	MDCK	Pgp-inh	Pgp-sub	HIA	F (20%)
442824	-4.807	1.78E-05	0.274	0.002	0.021	0.002
107935	-4.952	2.42E-05	0.999	0	0.009	0.009
156341	-4.725	4.36E-05	0.999	0	0.006	0.005
182678	-4.725	4.36E-05	0.999	0	0.006	0.005

3083803	-4.869	2.85E-05	0.998	0.001	0.010	0.003
44257420	-4.760	2.22E-05	0.351	0.006	0.005	0.003
6758	-4.860	2.80E-05	0.872	0.001	0.007	0.002
10177	-4.947	1.58E-05	0.006	0	0.010	0.015
114909	-4.819	2.24E-05	0.997	0	0.014	0.008
5280445	-5.028	1.00E-05	0.004	0.274	0.047	0.998
10215	-5.093	1.43E-05	0.045	0	0.007	0.004
5280863	-4.974	9.07E-06	0.004	0.011	0.008	0.856
5280443	-4.847	1.16E-05	0.004	0.820	0.015	0.995
439336	-6.235	0.000687522	0.001	0.890	0.999	0.980
441564	-5.230	4.06E-05	0	0.093	0.798	0.018

Table 5. Distribution properties of the top 15 ligands.

PubChem CID	PPB	VDss	BBB	Fu
442824	97.56%	0.529	0.014	2.39%
107935	99.55%	0.561	0.063	2.41%
156341	89.03%	1.580	0.048	8.09%
182678	89.03%	1.580	0.048	8.09%
3083803	89.69%	0.629	0.048	8.18%
44257420	99.75%	0.509	0.029	1.24%
6758	97.78%	0.594	0.094	2.41%
10177	98.74%	0.367	0.348	1.16%
114909	93.53%	0.945	0.197	8.26%
5280445	95.44%	0.533	0.009	5.98%
10215	99.50%	0.384	0.359	1.16%
5280863	97.86%	0.522	0.009	4.41%
5280443	97.25%	0.510	0.012	3.67%
439336	10.43%	0.189	0.417	59.63%
441564	36.23%	0.652	0.616	57.69%

Table 6. Metabolism and excretion properties of the top 15 ligands.

PubChem CID	CYP1A2-inh	CYP1A2-sub	CYP3A4-inh	CYP3A4-sub	CL	T12
442824	0.098	0.843	0.865	0.708	7.89	0.074
107935	0.269	0.882	0.947	0.750	3.417	0.084
156341	0.121	0.213	0.152	0.228	1.647	0.087
182678	0.121	0.213	0.152	0.228	1.647	0.087
3083803	0.363	0.963	0.553	0.566	2.561	0.237
44257420	0.233	0.961	0.789	0.836	9.560	0.136
6758	0.083	0.918	0.904	0.797	8.285	0.069
10177	0.982	0.808	0.448	0.355	0.795	0.135
114909	0.223	0.756	0.857	0.884	3.703	0.118
5280445	0.981	0.154	0.549	0.092	8.146	0.898
10215	0.978	0.871	0.448	0.596	0.625	0.155
5280863	0.972	0.110	0.697	0.080	6.868	0.905
5280443	0.988	0.145	0.833	0.126	7.022	0.856
439336	0	0.006	0.001	0	0.767	0.537
441564	0.072	0.076	0.009	0.039	2.257	0.565

Table 7. Toxicity properties of the top 15 ligands.

PubChem CID	hERG	H-HT	DILI	Ames	Carcinogenicity	Respiratory	IGC50	LC50
442824	0.049	0.242	0.628	0.122	0.156	0.791	4.963	7.644
107935	0.111	0.807	0.659	0.229	0.769	0.869	4.820	7.135
156341	0.012	0.663	0.966	0.800	0.787	0.328	4.788	7.279
182678	0.012	0.663	0.966	0.800	0.787	0.328	4.788	7.279
3083803	0.017	0.995	0.983	0.684	0.883	0.859	4.624	6.952
44257420	0.048	0.556	0.613	0.246	0.326	0.775	5.025	7.149
6758	0.072	0.249	0.722	0.283	0.280	0.785	5.004	7.915
10177	0.050	0.699	0.986	0.341	0.539	0.652	4.550	5.211
114909	0.285	0.833	0.132	0.230	0.897	0.534	4.219	6.090
5280445	0.064	0.084	0.905	0.536	0.095	0.220	4.432	5.222
10215	0.023	0.468	0.973	0.617	0.501	0.882	4.709	5.364
5280863	0.070	0.098	0.979	0.672	0.097	0.090	4.386	5.223
5280443	0.057	0.072	0.854	0.475	0.277	0.266	4.588	5.208
439336	0.054	0.053	0.103	0.105	0.008	0.005	1.945	0.324
441564	0.024	0.067	0.656	0.272	0.155	0.251	2.883	3.256

DISCUSSION

Prostate cancer is one of the most common types of malignancies, diagnosed in men. It results from the different environmental factors, diet, age, and family history of the disease [21, 22]. The diagnosis of this cancer can be done by blood tests such as prostate specific antigen (PSA) test, digital rectal exam, biopsy, etc. The treatment of prostate cancer depends on the extent of its spread. There are no proven medicines that can help in curing the disease yet, but surgery and radiation therapy can be done to improve the survival rate of the person [23]. Different pathway proteins are involved in the progression of prostate cancer such as epidermal growth factors (EGFR) and fibroblast growth factors (FGFR) [24]. These proteins have a series of signaling pathways that are involved in the progression of cancer. Thus, targeting these proteins for the anti-cancer treatment can be promising.

In this study, 4 proteins, (EGFR, ERK, FGFR, and FGF) were taken as target proteins. The structures were viewed using BIOVIA Discovery. The purified proteins were subjected to pdb sum generation. The Ramachandran plot results suggested that all 4 selected proteins were good quality models and had most of their residues come under allowed regions. The secondary structure prediction of all the proteins was also done for the target proteins which had 324, 302, 344, and 136 residues respectively.

In Molecular Docking and Visualization among the 20 ligands screened, the top 6 ligands that had the lowest binding energy with the proteins namely 1M17, 4ZZM, 5B7V, and 2P23 respectively were selected. The visualization results showed the implication that Leu 694 and Val702 were the most prevalent amino acids involved in the binding with the ligand in the 1M17 protein. Val A.39 was common in binding with all the top ligands in 4ZZM protein, and Leu 162 was the common amino acid in 2P23 protein. As shown in Figure 6, Figure 8, and Figure 12, respectively.

ADMET analysis results showed that, pseudosemiglabrin and [(12S,15R,16R)-14,14-dimethyl-6-oxo-4-phenyl-3,11,13-trioxatetracyclo [8.6.0.02,7.012,16] hexadeca-1(10),2(7),4,8-tetraen-15-yl] acetate compound was found to be having best binding affinity with all the 4 target proteins that is, -9.3 and -9.1 respectively with the protein 1M17, -8.5 and -8.4 with 4ZZM protein, -10.8 and -10.1, respectively, with 5B7V protein and -8.2 with the 2P23 protein. These 2 compounds have 0 Lipinski rules violation, and 0 PAINS alert (Table 3). The pharmacokinetic properties suggested that these compounds have high GI absorption, Plasma protein binding was found to be less than 90% and thus can be used as a therapeutic drug (Table 5).

Apart from these 2 compounds, the other compounds such as Sumatrol (PubChem ID: 442824), Deguelin (PubChem ID: 107935), and Rotenol (PubChem ID: 44257420) showed the least binding affinity with the 3 target proteins, they are 1m17, 4zzm, and 5b7v. These compounds had 0 Lipinski's rule violation, and 0 PAINS alert, and were moderately soluble in water. The compound Sumatrol had high GI absorption and no blood–brain penetration. The other 2 compounds, Deguelin and Rotenol showed high GI absorption and blood–brain penetration (Table 6). The results of this study showed that the compounds, Pseudosemiglabrin, [(12S,15R,16R)-14,14-dimethyl-6-oxo-4-phenyl-3,11,13-trioxatetracyclo [8.6.0.02,7.012,16] hexadeca-1(10),2(7),4,8-tetraen-15-yl] acetate, Deguelin, Sumatrol and Rotenone showed good binding affinity with the target proteins and can be considered as a potential drug for the prostate cancer.

CONCLUSION

As plant-derived compounds (herbal medicines) are becoming the trend, because of their long history of improving human health and being the cure for many diseases, *Indigofera tinctoria* proves to be a promising plant with its anti-cancerous properties, can be used as a remedy for prostate cancer. The 4 different pathway proteins involved in the disease were selected and docked against the 20 ligands from the plant. The top 6 ligands selected for each protein, with the least binding affinity, were visualized. The ADMET analysis suggested that the top selected compounds have 0 Lipinski rule violations and showed good results as anti-cancer drugs. Compounds such as pseudosemiglabrin, deguelin, and Rotenol have already been studied for their anti-cancerous properties but their implication in prostate cancer can be helpful in the treatment of the disease.

Acknowledgment

I would like to thank Ms. Susha Dinesh for her guidance in the current study. I thank BioNome (*https://bionome.in/*) for offering the computational facilities and help in scientific research.

Abbreviations

EGFR:	Epidermal Growth Factor Receptor
ERK:	Extracellular-signal regulated kinase
FGFR:	Fibroblast Growth Factor Receptor
FGF:	Fibroblast Growth Factor
PDB:	Protein Data Bank
GLOBOCAN:	Global Cancer Observatory
RTK:	Receptor Tyrosine Kinases
MAPK:	Mitogen-Activated Protein Kinase
HSPG:	Heparin Sulphate Proteoglycans
IMMPAT**:**	Indian Medicinal Plants, Phytochemistry And Therapeutics
RMSD:	Root Mean Square Deviation

REFERENCES

1. Rawla P. Epidemiology of prostate cancer. World J Oncol. 2019;10(2):63–89. doi: 10.14740/wjon1191.
2. Xie Y, Su N, Yang J, Tan Q, Huang S, Jin M et al. FGF/FGFR signaling in health and disease. Signal Transduct Target Ther. 2020;5(1):181. doi: 10.1038/s41392–020–00222–7.
3. Normanno N, De Luca A, Bianco C, Strizzi L, Mancino M, Maiello MR et al. Epidermal growth factor receptor (EGFR) signaling in cancer. Gene. 2006;366(1):2–16. doi: 10.1016/j.gene.2005.10.018.
4. Uribe ML, Marrocco I, Yarden Y. EGFR in cancer: signaling mechanisms, drugs, and acquired resistance. Cancers. 2021;13(11):2748. doi: 10.3390/cancers13112748.
5. Giacomini A, Grillo E, Rezzola S, Ribatti D, Rusnati M, Ronca R et al. The FGF/FGFR system in the physiopathology of the prostate gland. Physiol Rev. 2021;101(2):569–610. doi: 10.1152/physrev.00005.2020.

6. Chen KL, Chang WSW, Cheung CHA, Lin CC, Huang CC, Yang YN et al. Targeting cathepsin S induces tumor cell autophagy via the EGFR–ERK signaling pathway. Cancer Lett. 2012;317(1):89–98. doi: 10.1016/j.canlet.2011.11.015.
7. Itoh N, Ornitz DM. Evolution of the Fgf and Fgfr gene families. Trends Genet. 2004;20(11):563–9. doi: 10.1016/j.tig.2004.08.007.
8. Lu Y, Liu B, Liu Y, Yu X, Cheng G. Dual effects of active ERK in cancer: A potential target for enhancing radiosensitivity. Oncol Lett. 2020;20(2):993–1000. doi: 10.3892/ol.2020.11684.
9. Motamarri NS, Karthikeyan M, Rajasekar S, Gopal V. Indigofera tinctoria Linn-a phytopharmacological review. Int J Res Pharm Biomed Sci. 2012;3(1):164–9.
10. Thamilselvan V, Menon M, Thamilselvan S. Anticancer efficacy of deguelin in human prostate cancer cells targeting glycogen synthase kinase-3 β/β-catenin pathway. Int J Cancer. 2011;129(12):2916–27. doi: 10.1002/ijc.25949.
11. Ahmed Hassan LE, Khadeer Ahamed MB, Abdul Majid AS, Iqbal MA, Al Suede FS, Haque RA et al. Crystal structure elucidation and anticancer studies of (-)-pseudosemiglabrin: a flavanone isolated from the aerial parts of Tephrosia apollinea. PLOS ONE. 2014;9(6):e90806. doi: 10.1371/journal.pone.0090806.
12. Gerhäuser C, Mar W, Lee SK, Suh N, Luo Y, Kosmeder J et al. Rotenoids mediate potent cancer chemopreventive activity through transcriptional regulation of ornithine decarboxylase. Nat Med. 1995;1(3):260–6. doi: 10.1038/nm0395–260.
13. Wei YF, Su J, Deng ZL, Zhu C, Yuan L, Lu ZJ, Zhu QY. [Indirubin inhibits the proliferation of prostate cancer PC-3 cells]. Zhonghua Nan Ke Xue. 2015 Sep;21(9):788–91. Chinese.
14. Choi S, Choi Y, Dat NT, Hwangbo C, Lee JJ, Lee JH. Tephrosin induces internalization and degradation of EGFR and ErbB2 in HT-29 human colon cancer cells. Cancer Lett. 2010;293(1):23–30. doi: 10.1016/j.canlet.2009.12.012.
15. Da J, Xu M, Wang Y, Li W, Lu M, Wang Z. Kaempferol promotes apoptosis while inhibiting cell proliferation via androgen-dependent pathway and suppressing vasculogenic mimicry and invasion in prostate cancer. Anal Cell Pathol (Amst). 2019;2019:1907698. doi: 10.1155/2019/1907698.
16. Orton RJ, Adriaens ME, Gormand A, Sturm OE, Kolch W, Gilbert DR. Computational modelling of cancerous mutations in the EGFR/ERK signalling pathway. BMC Syst Biol. 2009;3(1):100. doi: 10.1186/1752–0509–3–100.
17. Renukadevi KP, Sultana SS. Determination of antibacterial, antioxidant and cytotoxicity effect of Indigofera tinctoria on lung cancer cell line NCI-h69. Int J Pharmacol. 2011;7(3):356–62. doi: 10.3923/ijp.2011.356.362.
18. Srinivasan N. Medicinal plants for cancer treatment: a review approach. Int J Biol, (Research). 2018;3(4):57–61.
19. Szymczyk J, Sluzalska KD, Materla I, Opalinski L, Otlewski J, Zakrzewska M. FGF/FGFR-dependent molecular mechanisms underlying anti-cancer drug resistance. Cancers. 2021;13(22):5796. doi: 10.3390/cancers13225796.
20. Xiong G, Wu Z, Yi J, Fu L, Yang Z, Hsieh C et al. ADMETlab 2.0: an integrated online platform for accurate and comprehensive predictions of ADMET properties. Nucleic Acids Res. 2021;49(W1):W5-W14. doi: 10.1093/nar/gkab255.
21. Pienta KJ, Esper PS. Risk factors for prostate cancer. Ann Intern Med. 1993;118(10):793–803. doi: 10.7326/0003–4819–118–10–199305150–00007.
22. Crawford ED. Epidemiology of prostate cancer. Urology. 2003;62(6):3–12. doi: 10.1016/j.urology.2003.10.013.
23. Litwin MS, Tan HJ. The diagnosis and treatment of prostate cancer: a review. JAMA. 2017;317(24):2532–42. doi: 10.1001/jama.2017.7248.
24. Pernar CH, Ebot EM, Wilson KM, Mucci LA. The epidemiology of prostate cancer. Cold Spring Harb Perspect Med. 2018;8(12):a030361. doi: 10.1101/cshperspect.a030361.

